Ultra-compact planoconcave zoned metallic lens based on the fishnet metamaterial

V. Pacheco-Peña, B. Orazbayev, V. Torres, M. Beruete, and M. Navarro-Cía

Citation: Appl. Phys. Lett. **103**, 183507 (2013); doi: 10.1063/1.4827876
View online: http://dx.doi.org/10.1063/1.4827876
View Table of Contents: http://apl.aip.org/resource/1/APPLAB/v103/i18
Published by the AIP Publishing LLC.

Ultra-compact planoconcave zoned metallic lens based on the fishnet metamaterial

V. Pacheco-Peña,[1,a)] B. Orazbayev,[1,b)] V. Torres,[1,c)] M. Beruete,[1,d)] and M. Navarro-Cía[2,3,4,e)]
[1]*TERALAB (MmW—THz—IR & Plasmonics Laboratory), Universidad Pública de Navarra, Campus Arrosadía, 31006 Pamplona, Spain*
[2]*Optical and Semiconductor Devices Group, Department of Electrical and Electronic Engineering, Imperial College London, London SW7 2BT, United Kingdom*
[3]*Centre for Plasmonics and Metamaterials, Imperial College London, London SW7 2AZ, United Kingdom*
[4]*Centre for Terahertz Science and Engineering, Imperial College London, London SW7 2AZ, United Kingdom*

(Received 20 August 2013; accepted 14 October 2013; published online 31 October 2013)

A $1.5\lambda_0$-thick planoconcave zoned lens based on the fishnet metamaterial is demonstrated experimentally at millimeter wavelengths. The zoning technique applied allows a volume reduction of 60% compared to a full fishnet metamaterial lens without any deterioration in performance. The structure is designed to exhibit an effective refractive index $n = -0.25$ at $f = 56.7$ GHz ($\lambda_0 = 5.29$ mm) with a focal length FL $= 47.62$ mm $= 9\lambda_0$. The experimental enhancement achieved is 11.1 dB, which is in good agreement with simulation and also with previous full fishnet metamaterial lenses and opens the door for integrated solutions. © *2013 AIP Publishing LLC*. [http://dx.doi.org/10.1063/1.4827876]

The metal-lens antenna designed by Kock in 1946[1] is considered as one of the precursors of artificial dielectrics.[2] Exploiting the effective refractive index of waveguide modes, positive but less than one ($0 < n < 1$) indexes can be obtained, which are not attainable with natural dielectrics. As a result of such indexes, the profile of those converging metallic lenses inspired by Kock's design is concave rather than the usual convex shape of conventional dielectric lenses.[1–4] Recently, several researchers have revisited this approach for artificial material lenses within the framework of metamaterials.[3–11]

Metamaterials have attracted the attention of scientific community in the last years because they make it possible to create arbitrarily tailored electromagnetic parameters such as less than unity or even negative values of permittivity (ε) and permeability (μ).[12,13] This freedom allows realizing the Veselago's negative refractive index (NRI) medium investigated theoretically in 1960s.[12] Among the large number of metamaterial structures reported in the last years, the fishnet metamaterial has proven to provide the best performance for high frequency and quasi-optical applications.[14–16] It is based on stacked subwavelength hole arrays (SSHAs), and its underlying physics is closely related to the extraordinary transmission phenomenon (ET).[17–20]

The field of lenses has benefited greatly from investigation on metamaterials. The required profile of a metamaterial lens is directly linked to the effective refractive index value of the host material by the general equation of a conical section.[1,4] Therefore, depending on the value of n, a converging lens would require different geometrical profiles such as ellipses, hyperbolas, and parabolas. Many NRI metamaterial lenses based on the classical arrangement of split ring resonators and wires with planoconcave[21] and cylindrical profiles[22] have been reported. However, the operation frequency of these lenses is limited to microwaves due to their increasing losses with frequency and saturation of the magnetic response.[23] The solution for higher frequencies is the use of the fishnet metamaterials.[4,8–10] It has been demonstrated that by designing a free-standing fishnet metamaterial with two in-plane periods, a very low-loss structure can be fabricated in the millimeter-wave range.[18] In addition, through manipulation of permittivity and permeability a good (ideally perfect) matching to free space can be obtained as we demonstrated previously using a plano-concave lens.[7]

A major drawback of the mentioned fishnet metamaterial lenses is the large volume occupied by the lens material and the consequent weight of the structure. To mitigate this problem, one can apply the zoning technique whereby parts of the lens are removed when their phase variation with respect to free-space propagation is an integer multiple of 2π.[1,24] This technique has been used occasionally for classical metallic lenses.[1] However, it has significant importance for microwave and optical dielectric lenses, which are widely known as Fresnel lenses,[25] and for X-rays dielectric lenses.[26] Note that this technique not only reduces volume and weight but also minimizes lens absorption, i.e., losses. The disadvantage of the zoning technique is that it narrows the bandwidth of operation.

In this paper, we exploit the zoning technique to propose an ultra-compact low-loss and low-weight fishnet metamaterial lens. Analytical design, simulation, and experimental results are presented. The lens is designed to operate at $f = 56.7$ GHz ($\lambda_0 = 5.29$ mm), where it behaves as an effective NRI medium $n = -0.25$, with a focal length (FL) of $9\lambda_0$. Note that the fishnet metamaterial lens is already inherently narrowband, and thus its bandwidth is not affected by the zoning technique.

The design and numerical analysis of the lens is made using the commercial software CST Microwave Studio™.

[a)]Electronic mail: victor.pacheco@unavarra.es
[b)]Electronic mail: b.orazbayev@unavarra.es
[c)]Electronic mail: victor.torres@unavarra.es
[d)]Electronic mail: miguel.beruete@unavarra.es
[e)]Electronic mail: m.navarro@imperial.ac.uk

To compute the effective refractive index of an infinite fishnet metamaterial, whose unit cell with dimensions is shown in Fig. 1(a), the eigen-mode solver of the software is used. For this simulation perfect electric conductor (PEC) is used because it is a good approximation for millimeter-waves. The resulting n for the fundamental band is presented in Fig. 1(a). The metamaterial has a strongly dispersive effective negative refractive index. At the design frequency $f = 56.7$ GHz ($\lambda_0 = 5.29$ mm), the effective refractive index is $n = -0.25$.

As mentioned in the introduction, to focus an incoming plane wave using a NRI medium, one needs a planoconcave or a biconcave profile. We opt to design a cylindrical planoconcave profile, using the zoning technique, to ease the assembly of the lens. The designed focal length is $\mathrm{FL} = 47.62 = 9\lambda_0$. The zoned lens procedure relies on sequentially removing material from the lens profile where phase variation with respect to free-space propagation is equal to integer multiples of 2π. This phase variation is achieved by reducing the profile each time a maximum thickness (t) is reached. This thickness can be mathematically calculated as follows:

$$t = \frac{\lambda_0}{1 - n}, \tag{1}$$

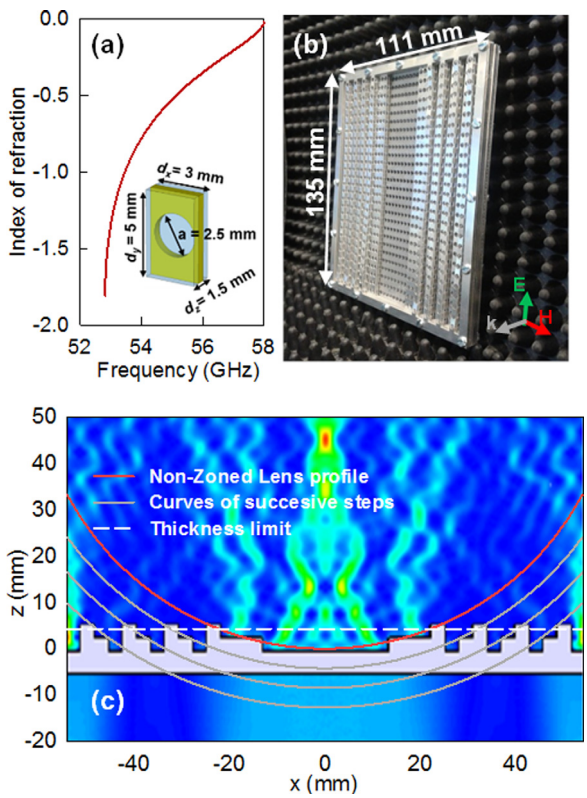

FIG. 1. (a) Index of refraction for a metamaterial made of an infinite number of SSHA. (Inset) Schematic representation of the unit cell with parameters: $d_x = 3$ mm, $d_y = 5$ mm, $d_z = 1.5$ mm, $a = 2.5$ mm, and metal thickness $w = 0.5$ mm. (b) Fabricated zoned fishnet metamaterial lens. (c) Lens profile: Non-zoned lens profile (red solid line), curves of the successive steps corresponding to the zoning technique (gray solid lines), and thickness limit t (white dashed line). Simulation results of the spatial power distribution on the xz-plane for a homogeneous material ($n = -0.25$) with the designed zoned lens profiled (background).

where λ_0 is the free-space wavelength and n is the index of refraction of the medium. According to this, the zoned lens is inevitably frequency-dependent in its behavior. However, this is not a drawback for metamaterial lenses since they are already narrowband. By combining fishnet metamaterial and the zoning lens techniques, it is possible to design compact lenses with a flat face and a zoned-stepped face at its input and output, respectively.

The zoned profile at the output of the structure is obtained by using the well-known general equation of an ellipse together with the condition maximum thickness defined by Eq. (1). The design equation is therefore

$$(1 - n_{lens}^2)(z + mt)^2 - 2(FL + mt)(1 - n_{lens})(z + mt) + x^2 = 0, \tag{2}$$

where n_{lens} is the effective refractive index of the structure, FL is the required focal length, m is an integer ($m = 0, 1, 2, 3$) and represent the successive steps for the zoned lens profile, and t is the thickness limit.[1,4]

The fabricated zoned fishnet metamaterial lens following the described design is shown in Fig. 1(b), and its final design profile is presented in Fig. 1(c) as a gray block along with the construction curves for $m = 0$, 1, 2, and 3. The red line corresponds to the profile of the lens when no zoning is applied, i.e., $m = 0$ in Eq. (2). The gray solid lines correspond to the successive profiles ($m = 1$, 2, 3). From Eq. (1) and the design wavelength ($\lambda_0 = 5.29$ mm), the maximum thickness is $t \approx 4.23\ \mathrm{mm} = 0.8\lambda_0$, which is plotted as a white horizontal dashed line. Note that each time the thickness limit is reached, the lens profile is reduced. By imposing t and the successive construction profiles, the final design needs 2 and 4 stacked perforated plates from the base line (i.e., central part of the lens) to map the zoned profile. The central part of the lens is made with 2 plates of holes. With these conditions, the zoned fishnet metamaterial lens is constructed with a total number of 37 and 27 holes along x and y directions, respectively, 2 and 6 plates are the minimum and maximum number of SSHAs used along z-axis. The whole structure, without the assembly frame, has maximum dimensions of $111 \times 135 \times 8$ mm ($21\lambda_0 \times 25.5\lambda_0 \times 1.5\lambda_0$).

The numerical analysis of the lens is made using the transient solver of the commercial software CST Microwave Studio™. Initially, we simulate a two-dimensional isotropic homogeneous lens with $n = -0.25$ and the designed stepping. This isotropic homogeneous lens will be used afterwards as a standard to evaluate the performance of the zoned fishnet metamaterial lens. The spatial power distribution on the xz-plane [Fig. 1(c)] demonstrates that the design behaves as a converging lens for the ideal case with the designed focal length $\mathrm{FL} = 47.6\ \mathrm{mm} = 9\lambda_0$.

For the rest of the simulations, a realistic three-dimensional fishnet metamaterial lens is modeled. The metal used for the zoned lens is aluminum with a conductivity $\sigma_{\mathrm{Al}} = 3.56 \times 10^7$ S/m. Given the twofold symmetry, magnetic and electric symmetries are used at yz- and xz-planes, respectively, in order to reduce computation effort, and perfectly matched layers are used for the rest of the simulation box boundaries. Hexahedral mesh with a resolution up to

$0.25\,\text{mm} \times 0.5\,\text{mm} \times 0.27\,\text{mm}$ is chosen to map accurately the geometry of the fishnet metamaterial lens. To find the FL from the simulation, a set of probes placed every 0.5 mm along the optical axis (from 20 mm to 70 mm from the center of the lens) is used. These probes record the waveforms at their positions and give the corresponding spectra by Fourier transformation. An impinging vertical polarized (E_y) plane-wave is used as a source exciting the structure from its planar face. The simulation is run for a sufficiently long time to ensure that the continuous-wave (CW) information obtained by Fourier transformations is valid.

Experimental measurements of the zoned lens are performed using an AB Millimetre™ quasi-optical vector network analyzer (VNA). A sketch of the experimental setup is presented in Fig. 2(a). A V-band corrugated horn antenna connected to the VNA is used as a feeder located 3300 mm away from the flat face of the zoned lens for quasi-plane-wave illumination. At this position the diameter of the beam waist of the Gaussian beam radiated by the corrugated horn antenna is ~1000 mm for the working wavelength (λ_0), around 10 times larger than the lens side. Hence, the whole fishnet metamaterial lens is uniformly illuminated. On the other side of the lens, an open-ended rectangular waveguide (WR-15) connected to the VNA is used as a detector. This waveguide is placed on an *xz* translation stage to scan the electric field along the *z*-axis from 20 to 70 mm away from the center of the lens in steps of 0.5 mm. Note that in the simulation the presence of the open-ended waveguide is not considered. In order to reduce diffraction and interferences by undesirable reflections, absorbers are used to cover the whole setup.

Simulation and experimental results of the power distribution *vs z*-axis and frequency are presented in Figs. 2(b) and 2(c), respectively. In general terms, the overall experimental *z*-frequency map resembles perfectly the simulation. In both color maps the peak of power (i.e., focus) happens at 56.7 GHz, which corresponds to the design frequency. However, the spatial position of the focus is slightly different. For the simulation, the peak of power is located at $z = 49.5\,\text{mm} = 9.35\lambda_0$ whereas it is $z = 46.5\,\text{mm} = 8.79\lambda_0$ for the experiment. To facilitate the comparison, the normalized power distribution along *z*-axis for both simulation and experimental cases at the design frequency 56.7 GHz is plotted together in Fig. 2(d). The small discrepancy can be attributed to the imperfections on the fabrication and assembly process. Moreover, note that both simulation and experimental FL are located at a distance close to the designed value ($9\lambda_0$). The depth of focus (DF), defined as the full with at half maximum along *z*-axis at the focal length, obtained from simulation and experiment is $11.16\,\text{mm} = 2.1\lambda_0$ and $17.8\,\text{mm} = 3.24\lambda_0$, respectively. The difference between these two results can be assigned to experimental tolerances such as the spatial averaging introduced by the non-ideal point detection performed with the open-ended waveguide. Meanwhile, the larger DF compared to the isotropic homogeneous case arises due to two reasons. On one hand, the fishnet metamaterial is anisotropic. On the other hand, the fishnet metamaterial effective refractive index displays dispersion with the number of SSHAs.[27] Increasing the number of SSHAs on the back of the lens would make it behave closer to the ideal condition,

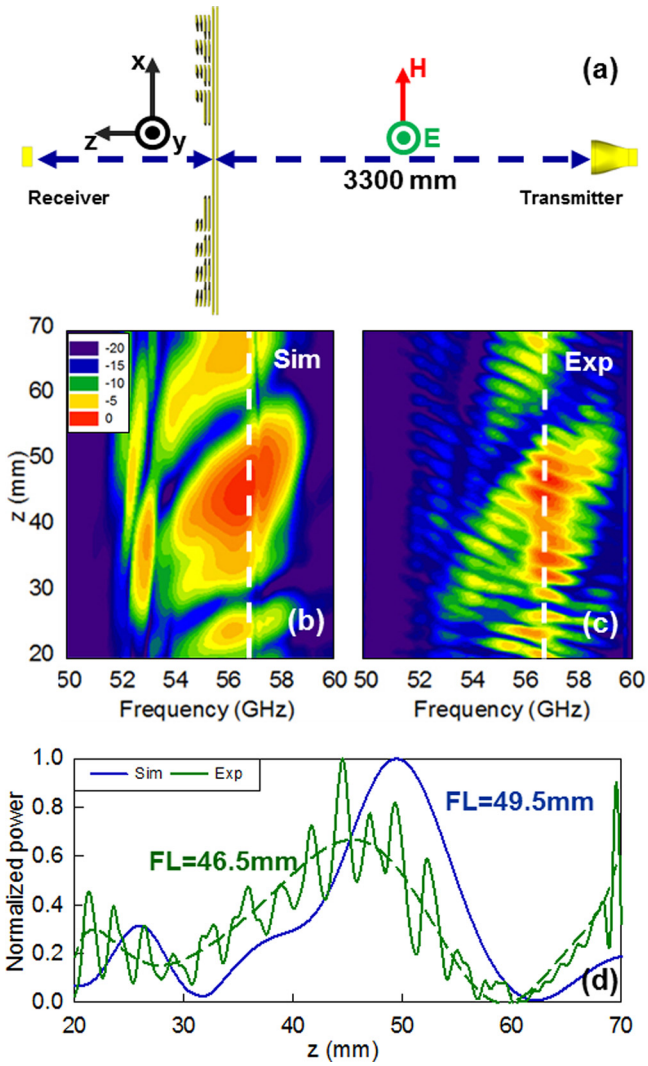

FIG. 2. (a) Schematic representation of the experimental set-up. Power distribution along *z* axis for the frequency range 50–60 GHz: (b) simulation and (c) experimental results. (d) Simulation and experimental results of the normalized power distribution along *z*-axis for the frequency $f = 56.7$ GHz.

but at the expense of increasing losses. Also, note that for the experimental case, ripples are present even when absorbers are used. It can be due to standing waves generated between receiver and the lens and appear for the whole range of frequency, see Fig. 2(c).

There is also a second peak of power in both color maps located at $z \sim 38$ mm and $f \sim 53$ GHz, with intensity ~5 dB lower than the main peak at 56.7 GHz. This secondary peak is related to the effective refractive index $n \approx -1.8$, which happens to require a similar, but obviously not identical, zoned profile. Moreover, it can be observed in both, simulation and experimental, cases that there is an absolute minimum at 60 GHz. This is related to the Wood's anomaly, which appears at $f = c/d_y = 60$ GHz.[28] According to the dispersion diagram, transmission through the fishnet metamaterial is prohibited below 52.3 GHz. This is demonstrated as well in both color maps where the detected power vanishes below 52 GHz for any *z*.

Next, the *xz*-plane is scanned experimentally with the open-ended waveguide. The scanning area comprises a square zone of the image plane going from 20 mm to 70 mm

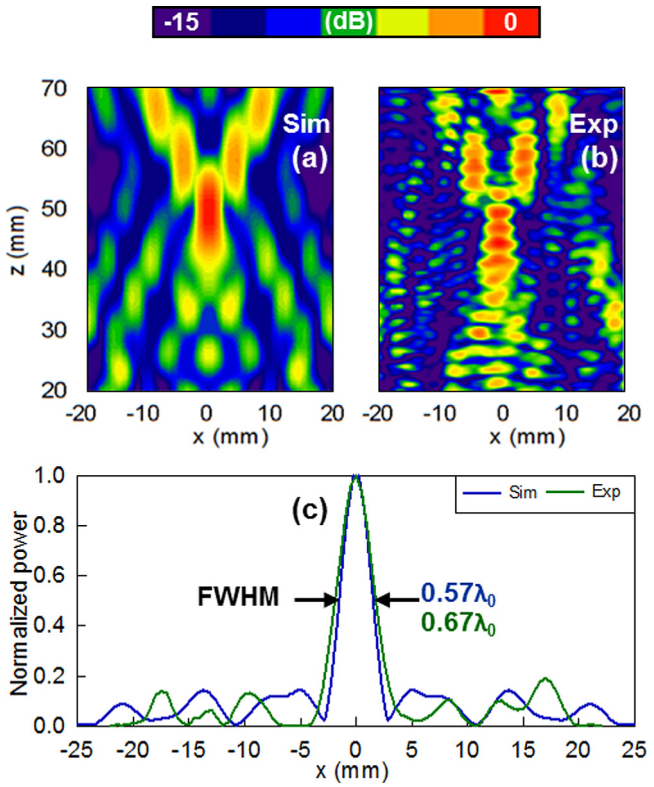

FIG. 3. Spatial power distribution in *xz*-plane: (a) simulation and (b) experimental results. (c) Simulation and experimental results of the normalized power distribution along *x*-axis.

in the *z* direction and from −20 mm up to 20 mm along the *x*-axis in steps of 0.5 mm. Simulation and experimental results of the normalized power distribution for the *xz*-plane are presented in Figs. 3(a) and 3(b), respectively. For the naked eye, it is evident the good agreement between simulation and experimental measurements with the same number of lateral side lobes in both cases. Furthermore, the maxima are clearly observed, and the small difference of the FL location is almost imperceptible for both simulation and experimental results.

From this *xz* scan we can estimate the remaining focal property, the full width at half maximum (FWHM). For clarity, we plot the power distribution along *x* at the focal length in Fig. 3(c). The FWHM values from simulation ($0.57\lambda_0$) and experimental measurements ($0.67\lambda_0$) are in good agreement with a small difference of $0.1\lambda_0 \approx 15\%$.

An important feature of the zoned fishnet metamaterial lens here presented is the enhancement observed at the focal length. Defining the enhancement as $T_{enh} = 10 \times \log_{10}(P_{R\_Lens}/P_{R\_free\text{-}space})$, where P_{R_Lens} is the received power with the lens and $P_{R\_free\text{-}space}$ the received power without the lens,[8] the zoned lens has an enhancement of 11 dB and 11.1 dB for simulation and experimental results, respectively, which is in agreement with previous designed planoconcave and biconcave lenses with parabolic profiles using fishnet metamaterial.[8–10]

To wrap up all the results presented here and facilitate the comparison among zoned and non-zoned lenses using the fishnet metamaterial and the isotropic homogeneous material with $n = -0.25$, simulation results for the FL, FWHM, DF, and the total volume for these three structures are presented in Table I along with the experimental results. It is shown that the resulting FL for the zoned lens $9.35(\lambda_0)$ is close to the values obtained with the non-zoned lens using fishnet metamaterial and the homogeneous medium, $8.96\lambda_0$ and $9.01\lambda_0$, respectively. As it has been explained before, the difference is due to the fact that the refractive index of the lens is dependent on the number of layers; hence, the FL of the non-zoned stepped lens is closer to the value obtained with an ideal isotropic homogeneous zoned lens with $n = -0.25$. Moreover, it can be observed that the FWHM values obtained with all the structures are similar. As for the depth of focus, it is smaller for the non-zoned lens using the fishnet metamaterial because the non-zoned lens has a larger numerical aperture, i.e., it accepts rays coming from larger angles. Finally, the reduction of volume by applying the zoning technique is approximately 60%. These results demonstrate that the zoned fishnet metamaterial lens is attractively compact, and its performance is competitive with non-zoned configurations and ideal homogeneous lenses.

In conclusion, a zoned cylindrical planoconcave fishnet metamaterial lens working at millimeter wavelengths has been designed, fabricated and measured. Simulation and experimental results are in good agreement in terms of focal length position, full width at half maximum, and depth of focus. The enhancement achieved with this lens is 11.1 dB, which is in good agreement with simulation result and also with previous planoconcave and biconcave lenses using SSHAs. The advantage of the zoned lens here presented is the volume reduction of 60% compared with a non-zoned lens made with the fishnet metamaterial. The comparison between both structures and an ideal homogeneous lens with

TABLE I. Simulation and experimental results for different lens designs using fishnet metamaterial and homogeneous material along with experimental results.

Lens design	FL[a]	FWHM[b]	DF[c]	Volume (mm^3)
Zoned lens with homogeneous material with n = −0.25	$47.63\,mm \approx 9.01\lambda_0$	$2.96\,mm \approx 0.56\lambda_0$	$7.36\,mm \approx 1.39\lambda_0$	78 975
Non-zoned lens using fishnet metamaterial	$47.41\,mm \approx 8.96\lambda_0$	$2.47\,mm \approx 0.47\lambda_0$	$6.77\,mm \approx 1.27\lambda_0$	196 830
Zoned lens using fishnet metamaterial (simulation)	$49.5\,mm \approx 9.35\lambda_0$	$3.01\,mm \approx 0.57\lambda_0$	$11.16\,mm \approx 2.1\lambda_0$	78 975
Zoned lens using fishnet metamaterial (experimental)	$46.5\,mm \approx 8.79\lambda_0$	$3.54\,mm \approx 0.67\lambda_0$	$17.8\,mm \approx 3.24\lambda_0$	78 975

[a]FL is the focal length.
[b]FWHM is the full width at half maximum.
[c]DF is the depth of focus.

$n = -0.25$ has been presented in terms of FL, FWHM, and DF demonstrating that using the zoning technique does not deteriorate the performance of the lens. The lens here presented is an alternative to conventional binary zone plates, which, unlike the zoned fishnet lens, cannot be free-space matched and display dielectric losses arisen from the unavoidable sustaining substrate. The proposed fishnet lens could be used for integrated solution requiring high-frequency efficient compact lenses.

This work was supported in part by the Spanish Government under contract Consolider Engineering Metamaterials CSD2008-00066 and contract TEC2011-28664-C02-01. V.P.-P. was sponsored by Spanish Ministerio de Educación, Cultura y Deporte under Grant No. FPU AP-2012-3796. B.O. was sponsored by Spanish Ministerio de Economía y Competitividad under Grant No. FPI BES-2012-054909. V.T. is sponsored by the Universidad Pública de Navarra. M.B. is sponsored by the Spanish Government via RYC-2011-08221. M.N.-C. was supported by the Imperial College Junior Research Fellowship. In memoriam of Professor Mario Sorolla.

[1]W. E. Kock, Proc. IRE **34**, 828 (1946).
[2]R. E. Colling and F. J. Zucker, *Antenna Theory* (McGraw-Hill, New York, 1969).
[3]R. Mendis and D. M. Mittleman, IEEE TMTT **58**, 1993 (2010).
[4]M. Navarro-Cía, M. Beruete, I. Campillo, and M. Sorolla, IEEE Trans. Antennas Propag. **59**, 2141 (2011).
[5]J. Liu, R. Mendis, and D. M. Mittleman, Appl. Phys. Lett. **103**, 031104 (2013).
[6]L. Verslegers, P. B. Catrysse, Z. Yu, J. S. White, E. S. Barnard, M. L. Brongersma, and S. Fan, Nano Lett. **9**, 235 (2009).
[7]M. Navarro-Cía, M. Beruete, M. Sorolla, and N. Engheta, Phys. Rev. B **86**, 165130 (2012).
[8]M. Beruete, M. Navarro-Cía, M. Sorolla, and I. Campillo, Opt. Express **16**, 9677 (2008).
[9]M. Navarro-Cía, M. Beruete, M. Sorolla, and I. Campillo, Appl. Phys. Lett. **94**, 144107 (2009).
[10]M. Navarro-Cía, M. Beruete, I. Campillo, and M. Sorolla, Phys. Rev. B **83**, 115112 (2011).
[11]V. Torres, V. Pacheco-Peña, P. Rodríguez-Ulibarri, M. Navarro-Cía, M. Beruete, M. Sorolla, and N. Engheta, Opt. Express **21**, 9156 (2013).
[12]V. G. Veselago, Sov. Phys. Usp. **10**, 509 (1968).
[13]L. Solymar and E. Shamonina, *Waves in Metamaterials* (Oxford University Press, New York, 2009).
[14]C. M. Soukoulis and M. Wegener, Nat. Photonics **5**, 523 (2011).
[15]S. Zhang, W. Fan, N. C. Panoiu, K. J. Malloy, R. M. Osgood, and S. R. J. Brueck, Phys. Rev. Lett. **95**, 137404 (2005).
[16]G. Dolling, C. Enkrich, M. Wegener, C. M. Soukoulis, and S. Linden, Science **312**, 892 (2006).
[17]M. Beruete, M. Sorolla, and I. Campillo, Opt. Express **14**, 5445 (2006).
[18]M. Navarro-Cía, M. Beruete, M. Sorolla, and I. Campillo, Opt. Express **16**, 560 (2008).
[19]R. Ortuño, C. García-Meca, F. J. Rodríguez-Fortuño, J. Martí, and A. Martínez, Phys. Rev. B **79**, 075425 (2009).
[20]V. Torres, P. Rodríguez-Ulibarri, M. Navarro-Cía, and M. Beruete, Appl. Phys. Lett. **101**, 244101 (2012).
[21]C. G. Parazzoli, R. B. Greegor, J. A. Nielsen, M. A. Thompson, K. Li, A. M. Vetter, M. H. Tanielian, and D. C. Vier, Appl. Phys. Lett. **84**, 3232 (2004).
[22]R. B. Greegor, C. G. Parazzoli, J. A. Nielsen, M. A. Thompson, M. H. Tanielian, and D. R. Smith, Appl. Phys. Lett. **87**, 091114 (2005).
[23]J. Zhou, T. Koschny, M. Kafesaki, E. N. Economou, J. B. Pendry, and C. M. Soukoulis, Phys. Rev. Lett. **95**, 223902 (2005).
[24]P. F. Goldsmith, in *Third International Symposium Space Terahertz Technology* (1992), pp. 345–361.
[25]H. D. Hristov, *Fresnel Zones in Wireless Links, Zone Plate Lenses and Antennas* (Artech House, Inc., Norwood, MA, 2000).
[26]V. Aristov, M. Grigoriev, S. Kuznetsov, L. Shabelnikov, V. Yunkin, T. Weitkamp, C. Rau, I. Snigireva, A. Snigirev, M. Hoffmann, and E. Voges, Appl. Phys. Lett. **77**, 4058 (2000).
[27]M. Navarro-Cia, M. Beruete, M. Sorolla, and I. Campillo, Phys. B: Condens. Matter **405**, 2950 (2010).
[28]R. D. Wood, Phys. Rev. **48**, 928 (1935).